Nucleon-Nucleon Scattering Parameters from Final-State Interactions*

E. E. Gross, E. V. Hungerford,† and J. J. Malanify‡

Oak Ridge National Laboratory, Oak Ridge, Tennessee 37830

and

R. Woods

Los Alamos Scientific Laboratory, Los Alamos, New Mexico

(Received 12 December 1969)

The energy spectra of α particles were measured at 5° lab for the reaction ^{3}He(^{3}He, α)pp using a 20-MeV ^{3}He beam; at 5° and 8° lab for the reaction ^{3}He(t, α)np; and at 5°, 8°, and 10° lab for the reaction ^{3}H(t, α)nn using a 22-MeV triton beam. The 5° lab spectra corresponding to low relative energy in the unobserved two-nucleon system were well fitted with Watson-Migdal final-state-interaction theory for the following scattering lengths: $a_{pp}=-7.52\pm0.22$ F, $a_{np}=-21.5\pm2.3$ F, and $a_{nn}=-16.96\pm0.51$ F. Analyzing the change-symmetric reactions with the comparison method and using the accepted value for a_{pp}, we find $a_{nn}=-18.11\pm0.75$ F. When compared with Coulomb-corrected values of a_{pp}, these values of a_{nn} imply that nucleon-nucleon forces are charge-symmetric to better than 1%. In obtaining the scattering lengths, the effective range was fixed at $r_0=2.84$ F. Allowing both the effective range and scattering length to vary in the fitting procedure for the n-n final-state data, we find $a_{nn}=-17.4\pm1.8$ F and $(r_0)_{nn}=2.4\pm1.5$ F. If the n-n scattering length is fixed at the value -17.0 F, our data determine the effective range to be $(r_0)_{nn}=2.75\pm0.35$ F.

I. INTRODUCTION

THE question of charge independence of nuclear forces continues to engage the interest of theorists and experimentalists. The near equality of n-n and p-p interactions (charge symmetry) was initially suggested by Helsenberg and confirmed by a study of the ground states of mirror nuclei.[1] Johnson[2] extended this equality to excited states, an offspring of these studies being the very lively field of isobaric analog states. Analysis of low-energy p-p and n-p scattering data led[3] to the extension of this symmetry principle to include the n-p interaction in the $^1S_0$ state (charge independence). Lending additional support for the charge independence of the strong interaction were many beautiful experiments on the interaction of π mesons with nucleons.[4] The elegant schemes now used to systematize a host of new "elementary" particles are indebted to the successful application of rotational invariance in isotopic-spin space to the π-nucleon system. However, the most sensitive test of charge independence continues to come from a comparison of the $^1S_0$ scattering parameters for the nucleon-nucleon system. Comparison of nucleon-nucleon scattering parameters suffers on the theoretical side by the present impossibility of separating electromagnetic contributions in a model-independent way[5] and suffers on the experimental side by the absence of free neutron-neutron scattering results.

Heller *et al.*[6] have shown that, depending upon the details of the assumed nuclear potential, the Coulomb-corrected $^1S_0$ scattering length for two protons "a_{pp}" can have values ranging from -16.5 to -19.0 F. It would thus appear that a determination of the n-n $^1S_0$ scattering length a_{nn} to an accuracy of ±0.5 F would not only be important with regard to the question of charge symmetry, but would also be useful in eliminating certain forms for the nucleon-nucleon potential (assuming charge symmetry). Recently, however, Miller *et al.*[7] have shown that "a_{pp}" is rather model-independent provided the model used is adjusted to fit the 0–330-MeV $^1S_0$ p-p scattering data and that "a_{pp}" then lies in the range -17.25 to -17.58 F.

Lacking free neutron targets, experimentalists have concentrated on measuring the so-called final-state interaction effects of two neutrons in three-body final states as first suggested by Watson.[8] The reactions are of the type

$$A+B\rightarrow X+nn, \qquad (1)$$

where the n-n interaction makes its appearance through

* Research sponsored in part by the U.S. Atomic Energy Commission under contract with Union Carbide Corporation.

† Present address: Rice University, Houston, Tex.

‡ Present address: Los Alamos Scientific Laboratory, Los Alamos, N.M.

[1] W. Heisenberg, Z. Physik **77**, 1 (1932); E. Feenberg and E. P. Wigner, Phys. Rev. **51**, 95 (1937).

[2] V.R. Johnson, Phys. Rev. **86**, 302 (1952).

[3] G. Breit, E. U. Condon, and R. D. Present, Phys. Rev. **50**, 825 (1936).

[4] See, e.g., the review by Murray Gell-Mann and Kenneth M. Watson, Ann. Rev. Nucl. Sci. **4**, 219 (1954).

[5] J. D. Jackson and J. M. Blatt, Rev. Mod. Phys. **22**, 77 (1950).

[6] L. Heller, P. Signell, and N. R. Yoder, Phys. Rev. Letters **13**, 577 (1964).

[7] M. D. Miller, M. S. Sher, P. Signell, and N. R. Yoder, Phys. Letters **30B**, 157 (1969).

[8] Kenneth M. Watson, Phys. Rev. **88**, 1163 (1952).

an enhancement in the yield of X in those regions of phase space where the two neutrons are left with small relative momenta. In Watson's treatment, the reaction is separated into two steps, a short-ranged primary mechanism responsible for the formation of the final state followed by the final-state interaction of the two nucleons which is assumed to occur outside the initial interaction volume. This method was used to analyze[9] the forward-angle proton spectrum from the reaction[10] $^2\mathrm{H}(n, p)nn$ at 14 MeV to obtain a two-neutron scattering length $a_{nn}=-21.7\pm1$ F. Using the impulse approximation, Phillips[11] has extended Watson's treatment to "long-range" interactions which, when applied to the same reaction, yields a value[12] $a_{nn}=-14\pm3$ F. Slobodrian *et al.*,[13] using a comparison technique,[14,15] have recently reanalyzed all the $^2\mathrm{H}(n, p)nn$ data in a somewhat model-independent way by direct comparison to the $^2\mathrm{H}(p, n)pp$ reaction and show that the data are consistent with $a_{nn}=-16.7_{-3.0}{}^{+2.0}$ F. Both the Watson[8] and Phillips[11] treatments depend upon the assumption that the third-body yield is unaffected by possible interactions between the third body and one of the final-state nucleons. The comparison method presumably "corrects" for this defect in the theory provided that the final-state interaction n-X in Eq. (1) is identical to the final-state interaction p-$\bar{X}$, where $\bar{X}$ is the charge-symmetric nucleus of X. This is certainly the case for the reactions $^2\mathrm{H}(n, p)nn$ and $^2\mathrm{H}(p, n)pp$.

The comparison method has also been invoked for the analysis of the charge-symmetric reactions $^3\mathrm{He}(d, t)pp$ and $^3\mathrm{H}(d, {}^3\mathrm{He})nn$ near 30 MeV to give[15] $a_{nn}=-16.1\pm1.0$ F. This experiment is open to the criticism that the low-energy p-t interaction is known to differ substantially from that of n-^{3}He due to interference between Coulomb and nuclear forces.[16] However, there is no indication that these interactions seriously affect the data since the value of a_{pp} deduced by fitting the Watson theory to the triton spectra for the reaction $^3\mathrm{He}(d, t)pp$ is $a_{pp}=-7.69_{-0.67}{}^{+0.61}$ F at 30 MeV[15] and $a_{pp}=-7.3\pm0.6$ F at 36 MeV[17] in agreement with the value[18] -7.786 ± 0.008 F from free p-p scattering.

The reaction $^2\mathrm{H}(\pi^-, \gamma)nn$ appears to be the cleanest with regard to nucleon third-particle interactions since the third particle is a γ ray. This reaction, however, is not without theoretical difficulties[19] and the experimental difficulties have so far limited the determination of a_{nn} to ±1.9 F, the latest value reported[20] being $a_{nn}=-16.4\pm1.9$ F. An unpublished reanalysis of these data yields[21] $a_{nn}=-18.43\pm1.53$ F. Other determinations of a_{nn} by this reaction report values of $-15.1_{-3.3}{}^{+2.5}$ F[22] and $-13.1_{-3.4}{}^{+2.4}$ F.[23] Furthermore, the π^- capture experiment does not determine the sign of a_{nn} and shows very little sensitivity, if any, to the effective range r_0.[19]

Measurements of the reaction $^3\mathrm{He}(^3\mathrm{He}, \alpha)pp$ at 53 MeV[24] and at 43.7 and 53.0 MeV[25] have shown that the α-particle spectra are well represented by the Watson theory for the accepted value of a_{pp}. It is therefore suggestive that the charge-symmetric reaction $^3\mathrm{H}(t, \alpha)nn$ would be a promising one for a study of the n-n interaction. These reactions are also attractive from the viewpoint of the comparison technique since the low-energy p-α interaction is very similar to the low-energy n-α interaction.[26] Furthermore, by extending the comparison to include the reaction $^3\mathrm{He}(t, \alpha)np$, a test of charge independence becomes possible in addition to a test of the less-restrictive charge symmetry. Towards this end, we report in this paper α-particle spectra at 5°, 8°, and 10° lab for the reaction $^3\mathrm{H}(t, \alpha)nn$ with 22-MeV tritons; 5° and 8° lab α spectra for the reaction $^3\mathrm{He}(t, \alpha)np$ with 22-MeV tritons; and 5° lab α spectra for the reaction $^3\mathrm{He}(^3\mathrm{He}, \alpha)pp$ using a 20-MeV ^{3}He beam. We then analyze the 5° lab spectra (these have the best statistical accuracy) with the Watson theory[8] to extract two-nucleon scattering parameters.

II. EXPERIMENTAL DETAILS

The α-particle spectra reported and analyzed in this paper were obtained by use of broad-range magnetic spectrographs of the Elbek[27] type, together with nuclear emulsions as detectors. Details of the spectrograph facility used in conjunction with the ^{3}He beam (Oak Ridge Isochronous Cyclotron) may be found in Refs. 24 and 28. The triton-beam part of this experi-

[9] K. Ilakovac, L. G. Kuo, M. Petravic, I. Slaus, and P. Tomas, Phys. Rev. Letters **6,** 356 (1961).
[10] M. Cerineo, K. Ilakovac, I. Slaus, P. Tomas, and V. Valković, Phys. Rev. **133,** B948 (1964).
[11] R. J. N. Phillips, Nucl. Phys. **53,** 630 (1964).
[12] E. Bar-Avraham, R. Fox, Y. Porath, G. Adam, and G. Frieder, Nucl. Phys. **B1,** 49 (1967).
[13] R. J. Slobodrian, H. E. Conzett, and F. G. Resmini, Phys. Letters **27B,** 405 (1968).
[14] W. T. H. van Oers, I. Slaus, and T. A. Tombrello, Bull. Am. Phys. Soc. **10,** 693 (1965).
[15] E. Baumgartner, H. E. Conzett, E. Shield, and R. J. Slobodrian, Phys. Rev. Letters **16,** 105 (1966).
[16] I. Ya. Banit and V. A. Sergeev, Yadern. Fiz. **4,** 712 (1967) [English transl.: Soviet J. Nucl. Phys. **4,** 507 (1967)].
[17] B. J. Morton, E. E. Gross, J. J. Malanify, and A. Zucker, Phys. Rev. Letters **18,** 1007 (1967).
[18] R. J. Slobodrian, Phys. Rev. Letters **21,** 438 (1968).
[19] M. J. Maravcsik, Phys. Rev. **136,** B624 (1964).
[20] R. P. Haddock, R. M. Salter, Jr., M. Zeller, J. B. Czirr, and D. R. Nygren, Phys. Rev. Letters **14,** 318 (1965).
[21] D. R. Nygren (private communication).
[22] J. W. Ryan, Phys. Rev. Letters **12,** 564 (1964).
[23] P. G. Butler, N. Cohen, A. N. James, and J. P. Nicholson, Phys. Rev. Letters **21,** 470 (1968).
[24] B. J. Morton, E. E. Gross, E. V. Hungerford, J. J. Malanify, and A. Zucker, Phys. Rev. **169,** 825 (1968).
[25] R. J. Slobodrian, J. S. C. McKee, W. F. Tivol, D. J. Clark, and T. A. Tombrello, Phys. Letters **25B,** 19 (1967).
[26] D. C. Dodder and J. L. Gammel, Phys. Rev. **88,** 520 (1952); J. D. Seagrave, *ibid.* **92,** 1222 (1953).
[27] J. Borggren, B. Elbek, and L. P. Nielsen, Nucl. Instr. Methods **24,** 1 (1963).
[28] J. B. Ball, IEEE Trans. Nucl. Sci. **NS13,** 340 (1966).

ment was conducted at the Los Alamos Tandem and their spectrograph facility is described in Ref. 29.

The gas target used in the triton-beam experiments had 2.11-mg/cm^2 entrance and exit Havar windows and was filled with either 190 mm of ^{3}He (99.7 at.%) or 190 mm of tritium (92.1 at.% ^{3}H, 1.0 at.% ^{2}H, 6.7 at.% ^{1}H, 0.14 at.% ^{3}He) at 20°C. The ^{2}H contaminant in the tritium gas target proved very useful in providing energy resolution and absolute cross-section information by observation of the line from the reaction $^2\mathrm{H}(t,\alpha)n$. Energy resolution for the ^{3}He gas-target data was conveniently provided by observing the line from the reaction $^3\mathrm{He}(t,\alpha)d$.

The gas target used in the ^{3}He beam experiment had a 2.71-mg/cm^2 Be entrance window and a 2.11-mg/cm^2 Havar exit window. The target filling consisted of 294 mm of ^{3}He and 5 mm of ^{2}H and was cooled to liquid-nitrogen temperature. The small addition of ^{2}H allowed for a determination of the energy resolution and absolute cross section via the reaction $^2\mathrm{H}(^3\mathrm{He},\alpha)p$. Cryogenic cooling of the target effectively reduced room-temperature exposures by a factor of 4. Satisfactory window seals were achieved by epoxy bonding; other details of the cryogenic target are as reported elsewhere.[30]

Primary beam energies and energy spreads were determined by magnetic analysis and extrapolated to the center of the gas target by energy-loss and energy-straggling calculations. Table I contains the calculated beam energies at the center of the target for the three reactions studied. The c.m. energies in the final state for the charge-symmetric reactions $^3\mathrm{H}(t,\alpha)nn$ and $^3\mathrm{He}(^3\mathrm{He},\alpha)pp$ are within 358 keV of being identical. Also shown in Table I are the calculated α-particle resolutions at 5° lab for the three-body final-state reactions. These have been obtained from the measured resolutions of the α lines referred to above and then estimating the contributions to these resolutions by kinematic effects. Some exposures had to be repeated because reactions with unwanted oxygen and nitrogen contaminants placed lines in unfavorable positions.

TABLE I. Beam energies at the center of the target and α-particle resolutions for the reactions studied at 5° lab.

Reaction	Beam energy (MeV)	α resolution (keV)
$^3\mathrm{He}(^3\mathrm{He},\alpha)pp$	19.540	135
$^3\mathrm{He}(t,\alpha)np$	21.884	117
$^3\mathrm{H}(t,\alpha)nn$	21.879	117

However, these contaminant lines were useful in confirming energy resolution and absolute energy calculations. Of special importance here is the observed resolution for the line $^3\mathrm{He}(t,\alpha)d$, which has virtually the same kinematical contributions to energy resolution as the α particles from the three-body final state $^3\mathrm{He}(t,\alpha)np$. We believe the resolutions are known to ± 10 keV and absolute energies to ± 50 keV. Since the detailed shape of the final-state spectrum contains the information on the effective-range parameters, it should be emphasized that it is not only necessary to have the very best possible energy resolution but that the resolution must be accurately known.

III. DATA

A. $^3\mathrm{He}(^3\mathrm{He},\alpha)pp$, 5° lab

Figure 1 shows the raw emulsion data for the reaction $^3\mathrm{He}(^3\mathrm{He},\alpha)pp$ at 5° lab as the number of observed tracks per mm scanned. The line at 110 mm is due to α particles from the reaction $^2\mathrm{H}(^3\mathrm{He},\alpha)p$ from the small amount of deuterium added to the target for this purpose. α particles could not be separated from tritons or deuterons by grain density. A separate exposure with an aluminum absorber before the emulsion was made to determine the deuteron background and this is shown in Fig. 2. The sources of these deuterons are probably reactions with residual oxygen and nitrogen nuclei since reactions with ^{3}He or ^{2}H nuclei cannot contribute deuterons to the momentum region covered by the nuclear emulsion detector. The flat triton background shown in Fig. 2 came from a third exposure of small (2.5 cm×7.6 cm×50 μ thick) nuclear emulsions whose surfaces were aligned almost parallel to particle trajectories at the focal plane of the magnetic spectrometer. A 23-mg/cm^2 Al absorber before these plates reduced α-particle ranges to 200 μ and triton ranges to 140 μ. In this way, α particles and tritons could easily be separated by range in emulsion and the ratio of their yields was determined at several points along the focal plane. The triton background determined in this manner and properly normalized is as shown in Fig. 2. Subtraction of the deuteron and triton background results in the reduced α spectrum shown in Fig. 3 with typical statistical error bars indicated. The absolute cross-section scale is inferred from the observed number of α particles for the process $^2\mathrm{H}(^3\mathrm{He},\alpha)p$ and the reported[31] differential cross section for this reaction. We estimate the error on the absolute cross section to be about 25%. The horizontal scale has been converted to relative energy in the unobserved two-proton system by a knowledge of the magnet calibration[32] and kinematics calculations.

A further exposure was made at reduced magnetic

[29] G. Igo, P. D. Barnes, E. R. Flynn, and D. D. Armstrong, Phys. Rev. **177**, 1831 (1969).

[30] L. N. Blumberg, E. E. Gross, A. van der Woude, and A. Zucker, Nucl. Instr. Methods **39**, 125 (1966).

[31] L. Stewart, J. E. Brolley, and L. Rosen, Phys. Rev. **119**, 1649 (1960).

[32] J. B. Ball (private communication).

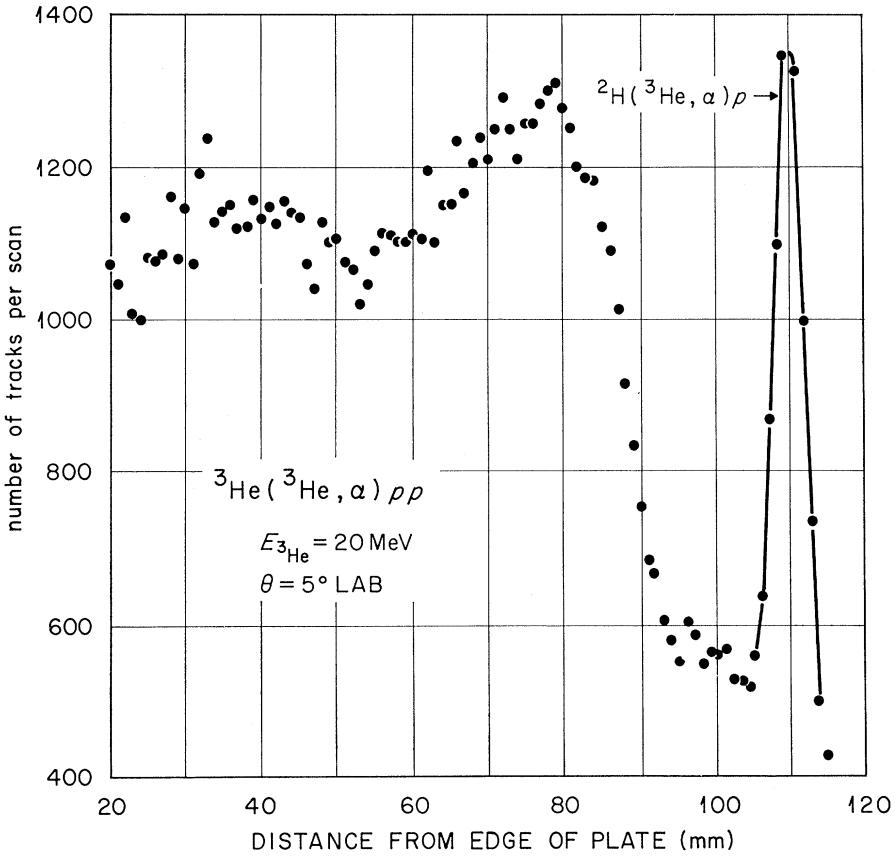

FIG. 1. Observed track distribution at 5° lab from the reaction $^3He+^3He$ for a 20-MeV ^3He beam. The line at 110 mm is due to α particles from the reaction $^2H(^3He, \alpha)p$. A small amount of deuterium was added to the target for this purpose.

field to determine the energy spectrum of ^3He particles at an energy of about 9 MeV from the processes $^3He(^3He, ^3He)dp$ and $^3He(^3He, ^3He)npp$. Under charge symmetry, this should be analogous to the spectrum of 9-MeV tritons from the processes $^3H(t, t)dn$ and $^3H(t, t)pnn$ which contribute a triton background to the final-state reaction of interest, $^3H(t, \alpha)nn$. The ~9-MeV ^3He particles are easily distinguished since their ranges are quite short. We found the ^3He spectrum to be flat to within 1% over the energy range of interest.

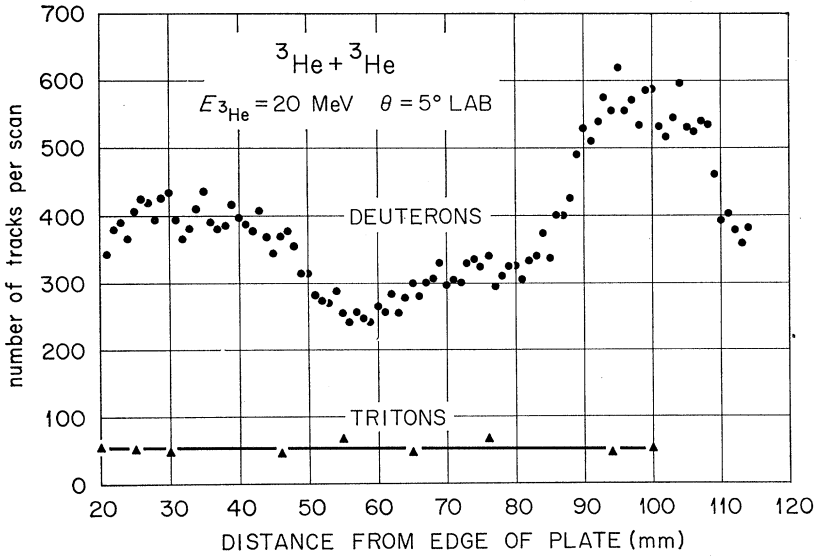

FIG. 2. Deuteron and triton contributions to the spectrum shown in Fig. 1. These were obtained in separate exposures as described in the text.

B. ^{3}He(t, α)np, 5° and 8° lab

The raw emulsion data for the reaction ^{3}He(t, α)np at 5° and 8° lab are shown in Fig. 4. We will concern ourselves exclusively with the 5° data which have much better statistical accuracy. The line at 136 mm corresponds to α particles leaving the final-state n-p system as a bound deuteron. The feature at about 95 mm is the characteristic final-state interaction peak leaving an unbound n-p system. This final-state peak is unfortunately partially obscured by another large peak at about 69 mm. An additional exposure with an absorber to remove α's and tritons reveals the peak at 69 mm to be composed of deuterons from the reaction ^{3}He(t, d)^{4}He* (20.3 MeV). The deuteron spectrum is shown in Fig. 5, from which we conclude an excitation energy of 20.05±0.08 MeV and a width of 0.36±0.08 MeV for this excited state of the α particle. These values are in agreement with the values reported by Jarmie *et al.*[33] who examined this same reaction at 10°, 15°, and 20° lab.

The relatively flat region between 100 and 130 mm in the 5° data of Fig. 4 is assumed to be a continuum of tritons from ^{3}He(t, t)ppn or ^{3}He(t, t)pd. That this region is predominantly tritons is borne out by a grain density study summarized in Fig. 6 and the deuteron exposure leading to Fig. 5 which revealed no deuterons above 85 mm. The various plate locations of Fig. 6 are also identified with the reaction assumed to contribute the dominating particle group and lends strong support, together with kinematics calculations, to our interpretation of the raw data in Fig. 4.

Subtracting the deuteron background of Fig. 5 and assuming a flat triton background we obtain a reduced α-particle spectrum for the reaction ^{3}He(t, α)np shown in Fig. 7. Typical statistical error bars are shown and the horizontal scale has been converted to relative energy in the unobserved n-p system using the magnet calibration.[29] The scatter in the data of Fig. 7 near 1.0 MeV occurs at the high-energy end of the deuteron background (Fig. 5) and indicates a slight mismatch in position for the exposures corresponding to Figs. 4 and 5.

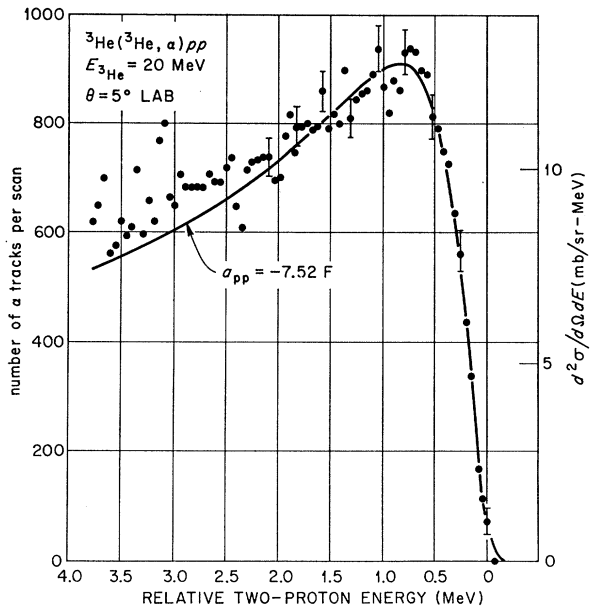

FIG. 3. Reduced α-particle spectrum for the reaction ^{3}He(^{3}He, α)pp at 5° lab to a 20-MeV ^{3}He beam. The horizontal scale has been converted to relative energy in the unobserved p-p system. The absolute differential cross-section scale is inferred from the observed reaction ^{2}H(^{3}He, α)p and the data of Ref. 31. The solid curve is the minimum χ^2 fit for $0 \leq E_{pp} \leq 2.0$ MeV.

C. ^{3}H(t, α)nn

The raw emulsion data for the reaction ^{3}H(t, α)nn at 5°, 8°, and 10° lab are shown in Fig. 8. Again we will concern ourselves almost exclusively with the more statistically significant 5° data. The line at 115 mm is attributed to the reaction ^{2}H(t, α)n from a small deuterium contamination in the tritium target. The strong line at 32 mm is due to the process ^{1}H(t, d)d from a larger hydrogen contamination in tritium gas. The striking feature at 80 mm is attributed to the sought after reaction ^{3}H(t, α)nn. Deuterons from reactions with ^{1}H, ^{2}H, or ^{3}H of the target cannot reach plate locations greater than 32 mm and a gap in the scanning between 38 and 50 mm (see Fig. 8) thus eliminates deuterons in the high-energy tail of ^{1}H(t, d)d from contaminating the 5° spectrum above 50 mm. The flat region between 90 and 110 mm is assumed to be a triton background from such processes as ^{3}H(t, t)nd and ^{3}H(t, t)nnp. This assumption, as well as the general interpretation of Fig. 8, is supported by the grain density distributions of Fig. 9 where the distributions are identified by location as well as by a reaction leading to the dominant group at that location. Further support comes from the corresponding ^{3}He background spectrum measured for the charge-symmetric processes ^{3}He(^{3}He, ^{3}He)pd and ^{3}He(^{3}He, ^{3}He)ppn which was found to be flat to within 1% as reported in Sec. III A.

Extending the assumed triton background between 90 and 100 mm to the region between 50 and 90 mm, we obtain the reduced α-particle spectrum shown in Fig. 10 as a function of the relative energy of the unobserved two-neutron system. The absolute differential cross-section scale comes from the cross section[34] for the process ^{2}H(t, α)n and the known concentration of

[33] N. Jarmie, R. H. Stokes, G. G. Ohlsen, and R. W. Newsome, Jr., Phys. Rev. **161**, 1050 (1967).

[34] J. E. Simmons and J. J. Malanify, Bull. Am. Phys. Soc. **13**, 564 (1968).

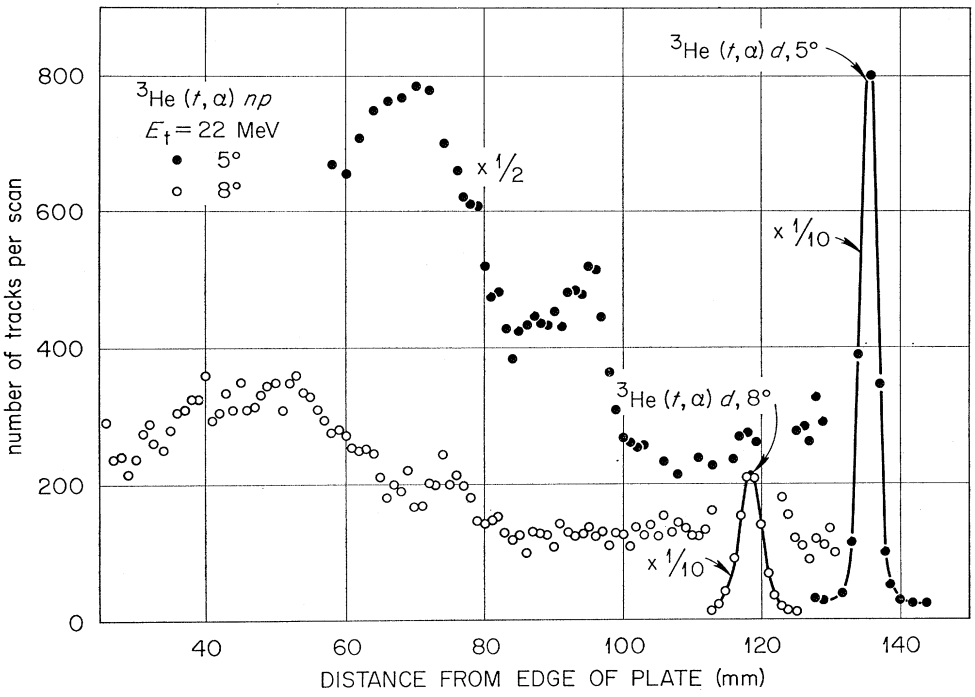

FIG. 4. Observed track distribution at 5° and 8° lab from the reaction $t+{}^3$He for a 22-MeV triton beam.

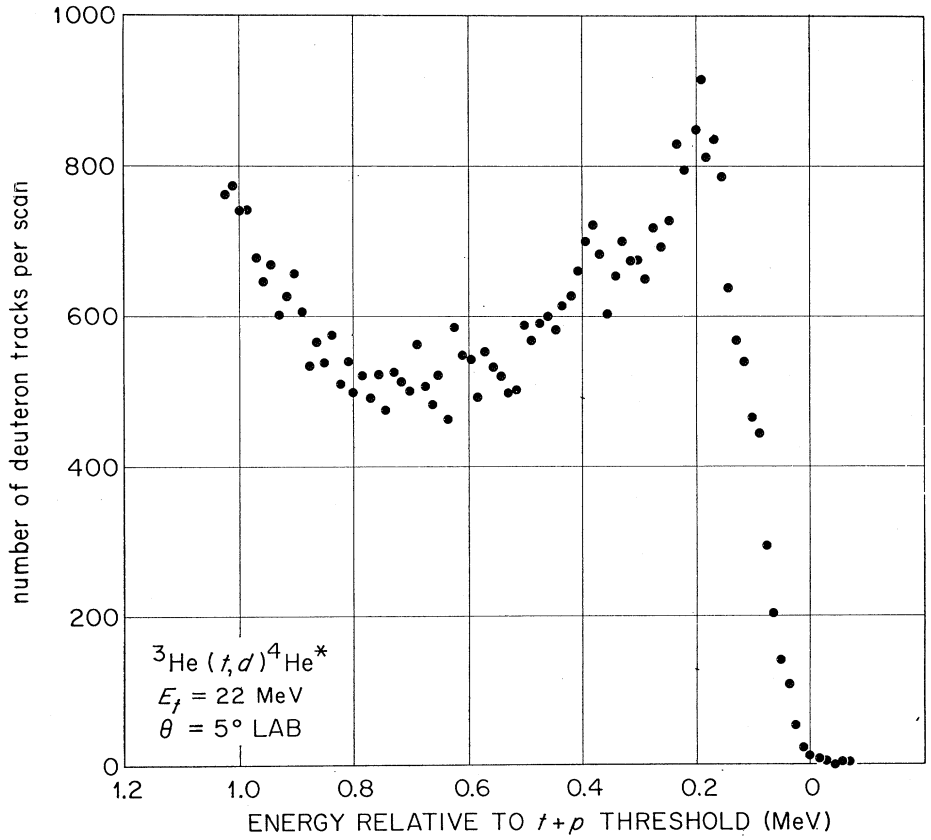

FIG. 5. Deuteron background contribution to the 5° lab spectrum of Fig. 4. The deuteron "peak" is ascribed to the process ^{3}He$(t,d)^4$He* (20.3 MeV).

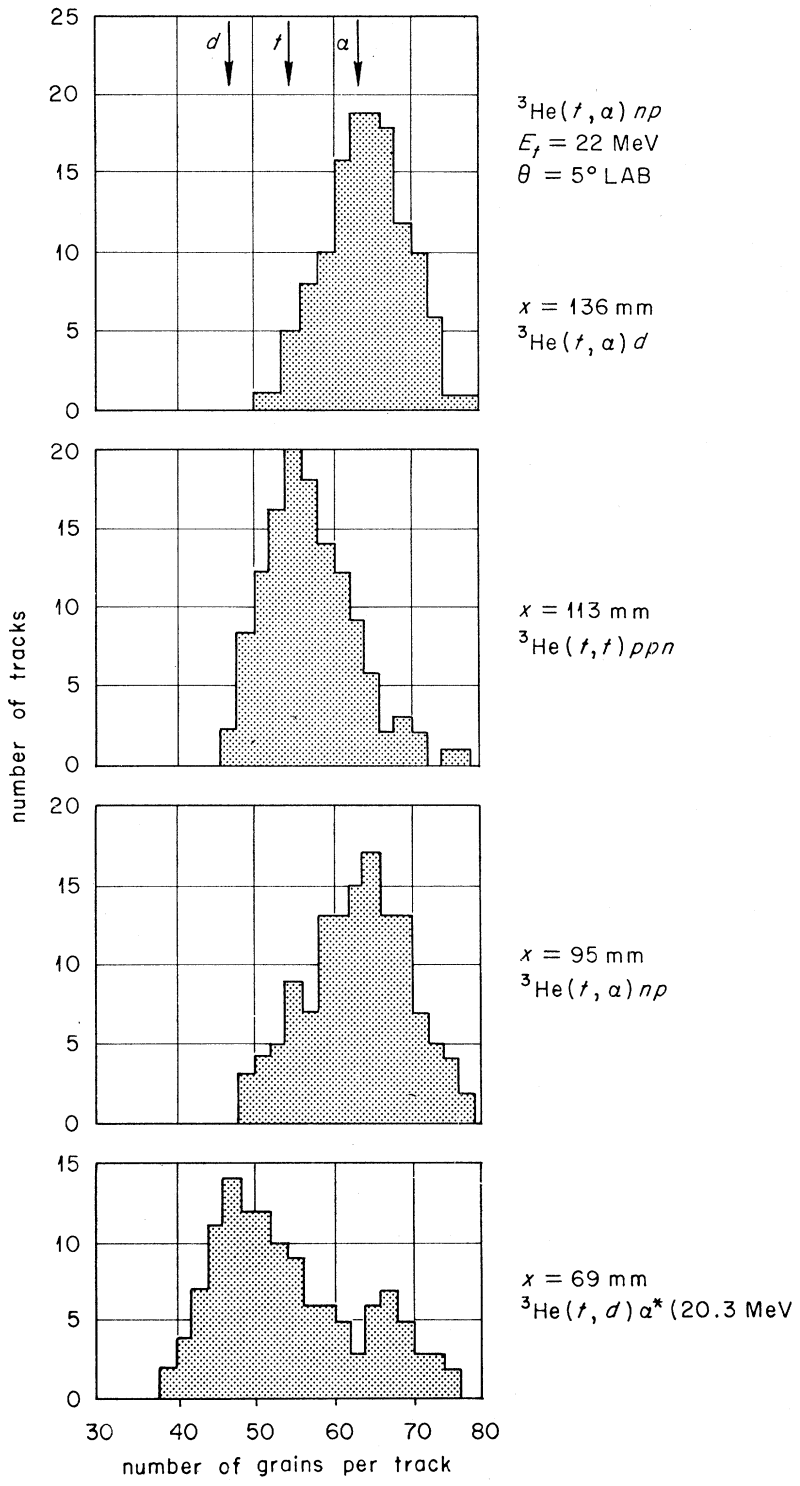

FIG. 6. Grain density distribution of tracks at the indicated plate positions. The plate positions refer to the 5° lab data of Fig. 4. Each distribution is also labeled by the reaction responsible for the prominent group of particles.

deuterium in the target on the same reaction and at the same energy. Typical statistical error bars are shown which assume the uncertainty in triton background to be determined by the *total* number of counts between 90 and 110 mm.

IV. ANALYSIS AND DISCUSSION

We take the view[8,35] here that the α-particle "peaks" of Figs. 3, 7, and 10 are manifestations of final-state

[35] W. T. H. van Oers and I. Slaus, Phys. Rev. **160**, 853 (1967).

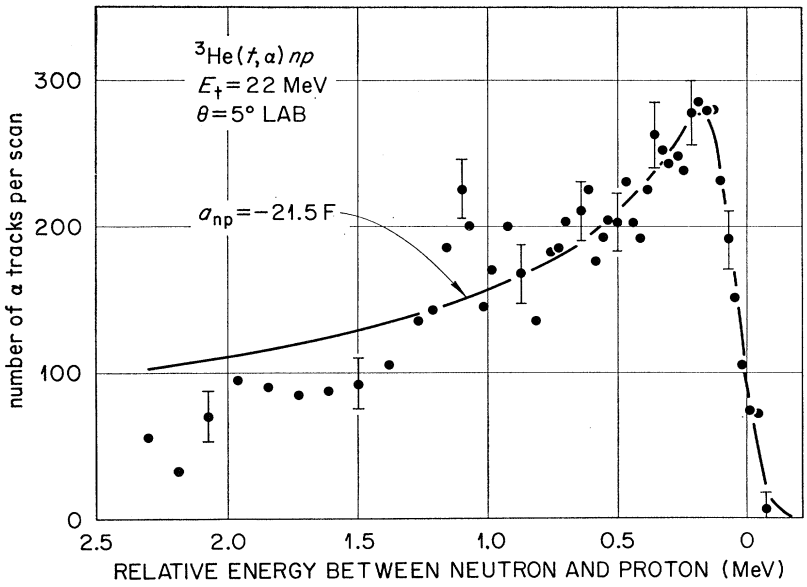

FIG. 7. Reduced α-particle spectrum for the reaction ^{3}He$(t, \alpha)np$ at 5° lab to a 22-MeV triton beam. The horizontal scale has been converted to relative energy in the unobserved n-p system. The solid curve is the minimum χ^2 fit for $0 \leq E_{np} \leq 1$ MeV.

S-wave interactions of the unobserved two-nucleon system. In this view, the final state is interpreted as a two-body final state consisting of an α particle and a di-nucleon system where the di-nucleon wave function ψ_{2N} is given by

$$\psi_{2N} = \exp(-i\delta)\, \sin(k_{2N}r+\delta)/k_{2N}r, \qquad (2)$$

for n-p or n-n systems or

$$\psi_{2N} = \exp(-i\delta)[F_0(k_{2N}r)\, \cos\delta + G_0(k_{2N}r)\, \sin\delta]/k_{2N}r, \qquad (3)$$

for the p-p system. In these expressions, k_{2N} is the relative momentum of the di-nucleon pair, r their separation, and δ is the S-wave phase shift. For the p-p system, F_0 and G_0 are the regular and irregular Coulomb wave functions, respectively. The final-state "peak" is thus a natural consequence of this interpretation and the shape of the "peak" is intimately related to the properties of the di-nucleon wave function.

Plausibility arguments for and against this interpretation are summarized in Ref. 35. As is pointed out there, and elsewhere,[14,15] performance and analysis of these reactions in charge-symmetric pairs offers the possibility of circumventing uncertainties regarding reaction mechanisms provided the assumptions[35] of the com-

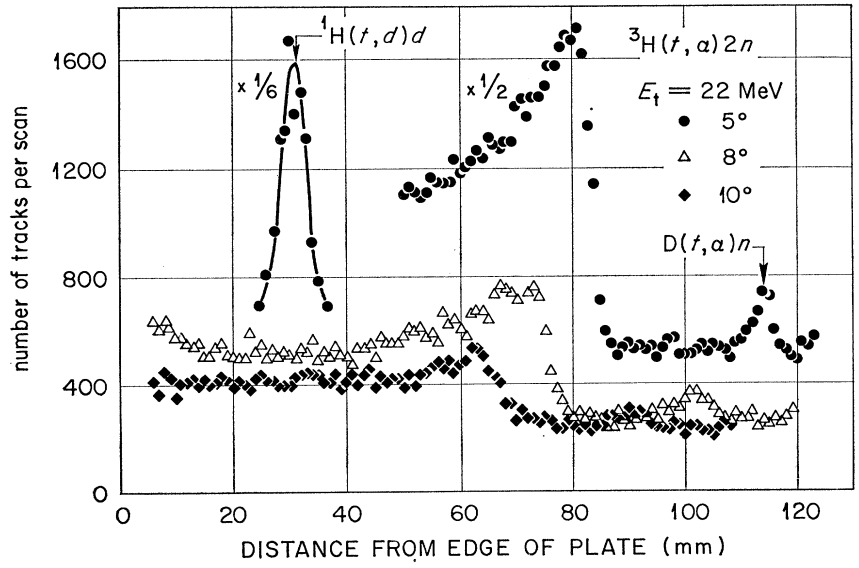

FIG. 8. Observed track distribution at 5°, 8°, and 10° lab from the reaction ^{3}H$(t, \alpha)nn$ for a 22-MeV triton beam. Shown in the 5° data is a strong deuteron line from a hydrogen contaminant and an α line from a deuterium contaminant.

parison method are valid. The di-proton member of the pair can lend further supporting evidence for the above interpretation if the deduced p-p parameters agree with those known from free p-p scattering. As we shall see below, the agreement is quite reasonable for the reactions studied here.

The general features of the analysis are set forth in detail in Ref. 24. For the pickup process assumed to be operative in our reactions, the short-range formulation of Watson[8] is most appropriate giving the laboratory differential cross section as

$$d^2\sigma/dE_\alpha d\Omega_\alpha \propto \frac{C^2(\eta)\rho(E_\alpha)}{C^4(\eta)E_{2N}+(\hbar^2/m)[-1/a_{2N}-H(\eta)/R+r_0 mE_{2N}/2\hbar^2]^2}. \quad (4)$$

In Eq. (4), $\rho(E_\alpha) \propto [E_\alpha(E_{\max}-E_\alpha)]^{1/2}$ is the phase space available to an α particle with energy E_α and $E_{\max}$ is the maximum kinetic energy allowable for the α particle. $C(\eta)=1$ for the np and nn final-state systems and is the Coulomb penetration factor for the pp system:

$$C^2(\eta)=2\pi\eta/[\exp(2\pi\eta)-1], \quad (5)$$

where

$$\eta=e^2/\hbar v_{2p} \quad (6)$$

and v_{2p} is the relative velocity of the two protons. $H(\eta)=0$ for the np and nn systems and is given by the following expression for the pp system:

$$H(\eta)=\mathrm{Re}[\Gamma'(-i\eta)/\Gamma(i\eta)]-\ln(\eta). \quad (7)$$

As shown by Migdal,[36] Eq. (4) results from Watson's[8] expression for the differential cross section when the phase shift δ is replaced by its effective-range expansion keeping terms up to second order in k_{2N}, a valid approximation for $E_{2N}\leq 2$ MeV. The effective-range theory parameters are the scattering length a_{2N} and the effective range r_0. Finally, m is the nucleon mass, $R=28.82$, and E_{2N} is the relative energy in the two-nucleon system.

In fitting Eq. (4) to the experimental data, we have folded in the experimental resolution and normalized the calculated spectrum to the number of observed α particles. The calculated spectrum appeared to be relatively insensitive to the effective range, especially for the p-p final state, and therefore we initially fixed the effective range at the value[18] $(r_0)_{2N}=2.84$ F. For a particular value of a_{2N}, the value of $E_{\max}$ was allowed to vary until

$$\chi^2=\sum_i [(N_{\mathrm{calc}}{}^i-N_{\mathrm{expt}}{}^i)/\Delta N_{\mathrm{expt}}{}^i]^2 \quad (8)$$

was minimized, where $N_{\mathrm{expt}}{}^i$ is the number of observed α particles at the ith position on the plate (i.e., the spectra of Figs. 3, 7, and 10), $\Delta N_{\mathrm{expt}}{}^i$ is the uncertainty in this number, and $N_{\mathrm{calc}}{}^i$ is the calculated number. Since we allow the normalization to vary, and allow the energy axis to slide, and search on a_{2N}, we estimate the number of degrees of freedom to be the number of data points minus three.

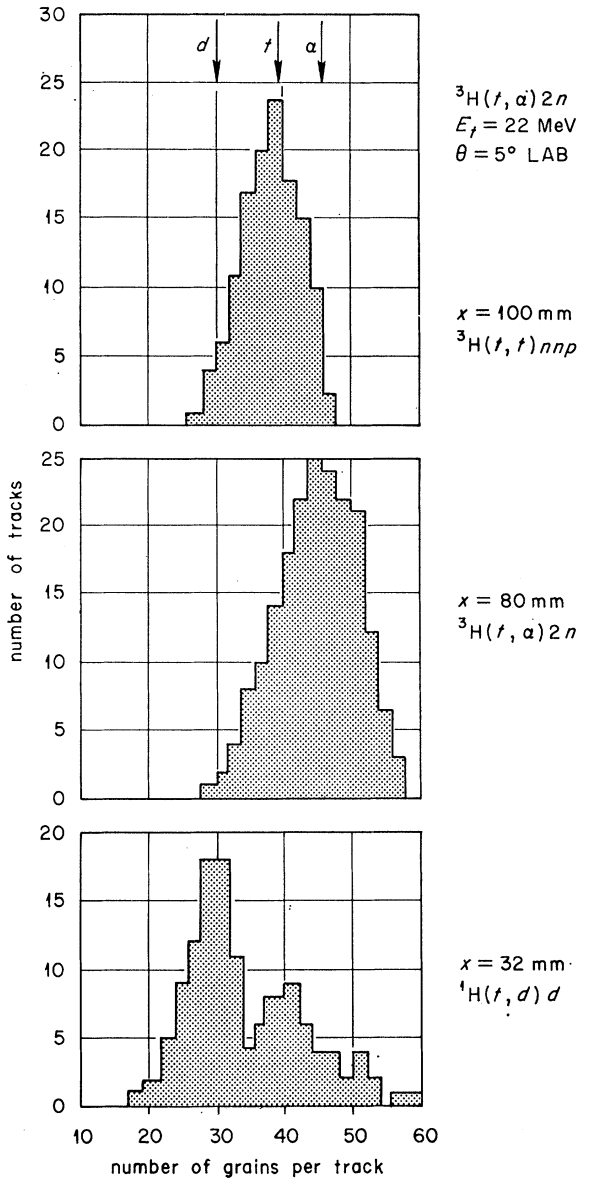

FIG. 9. Grain density distribution of tracks at the indicated plate positions. Plate positions refer to the 5° lab data of Fig. 8. Each distribution is labeled by the reaction responsible for the prominent group of particles.

[36] A. B. Migdal, Zh. Eksperim. i Teor. Fiz. **28**, 3 (1955).

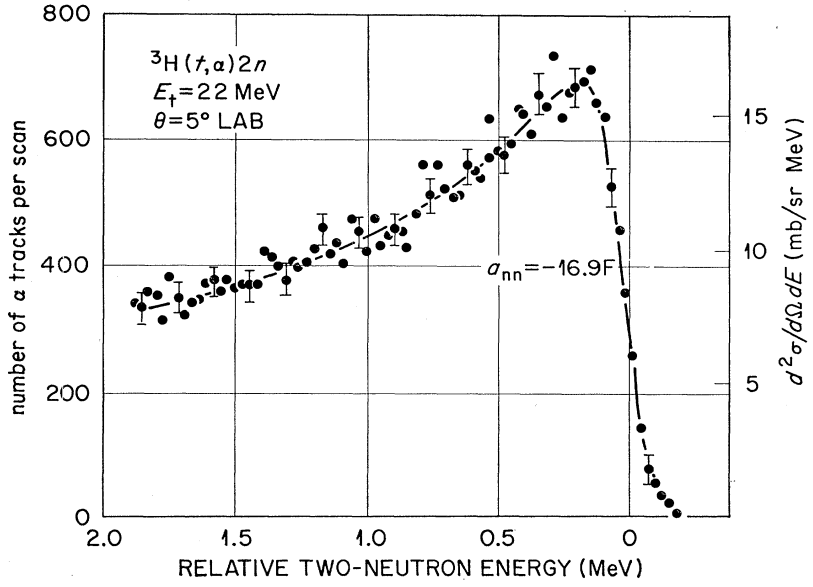

FIG. 10. Reduced α-particle spectrum for the reaction $^3H(t,\alpha)nn$ at 5° lab to a 22-MeV triton beam. The horizontal scale has been converted to relative energy in the unobserved n-n system. The absolute differential cross-section scale is based on the yield from $^2H(t,\alpha)n$ and the data of Ref. 34. The solid curve is the minimum χ^2 fit for $0 \leq E_{nn} \leq 1.9$ MeV.

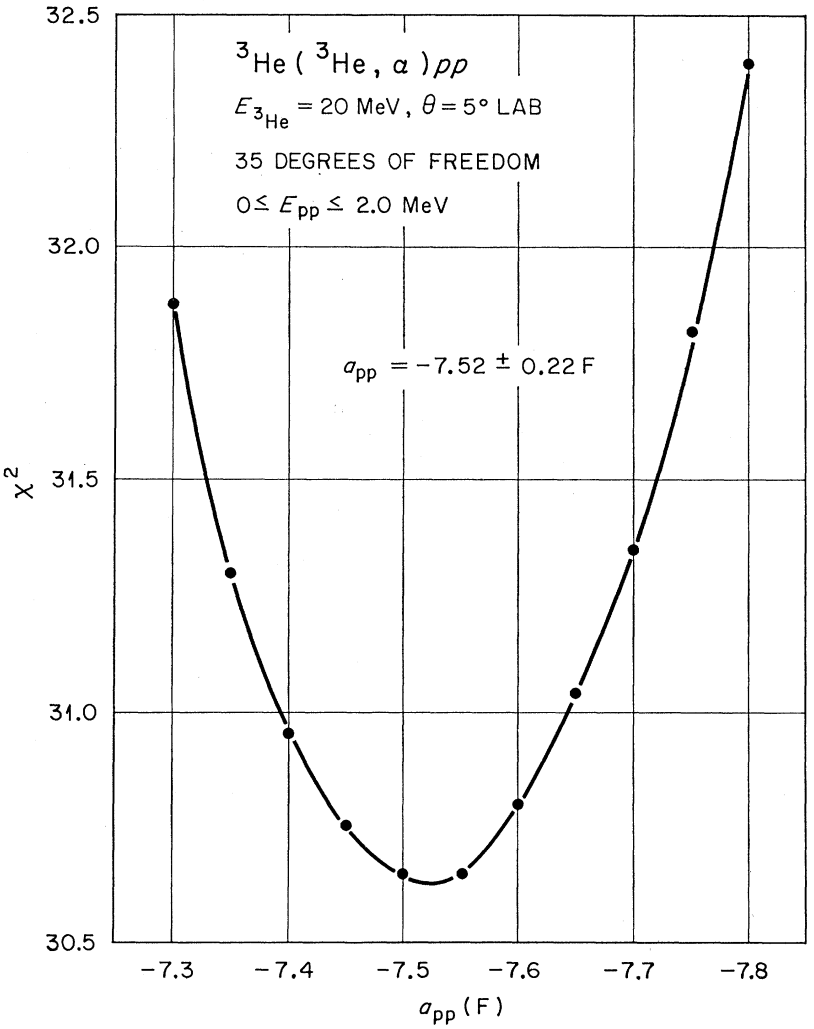

FIG. 11. χ^2 versus a_{pp} for the data of Fig. 3 in the range $0 \leq E_{pp} \leq 2$ MeV. The effective range has been fixed at $r_0 = 2.84$ F. At each value of a_{pp}, Eq. (4), including experimental resolution, was normalized to the total number of counts and the absolute energy allowed to shift until χ^2 was minimized.

A. ^{3}He(^{3}He, α)pp

The minimum χ^2 fit to the two-proton final-state data using the analysis procedure just described is shown as the solid curve in Fig. 3. The χ^2 surface as a function of two-proton scattering length a_{pp} is shown in Fig. 11. These calculations include the contribution to χ^2 due to an uncertainty in beam energy but not an uncertainty in effective range which has been fixed at the value 2.84 F. However, the $\chi_{\min}^2$ value of a_{pp} is quite insensitive to reasonable changes in $(r_0)_{pp}$, a 10% change in $(r_0)_{pp}$ is reflected in a 1% change in the value of a_{pp}.

The data being fit contain 35 degrees of freedom and we would therefore expect the minimum value of χ^2 to be $\chi_{\min}^2=35\pm6$. The value $\chi_{\min}^2=30.6$, together with the pleasing fit shown in Fig. 3, suggests that the theory offers a good representation of the data and that the errors assigned to the data points are reasonable. From Fig. 11, we find $a_{pp}=-7.52\pm0.22$ F, where the error limit is defined as the increment in a_{pp} required to increase $\chi_{\min}^2$ to $\chi_{\min}^2+1$. Both the value of a_{pp} and its uncertainty defined in this way are fairly insensitive to the assignment of errors on the data points, provided the errors are reasonably related to the statistics on the data points. The value $a_{pp}=-7.52\pm0.22$ F is only 0.04 F outside the error limits to agree with the value $a_{pp}=-7.786\pm0.008$ F given by a recent analysis[18] of free p-p scattering.

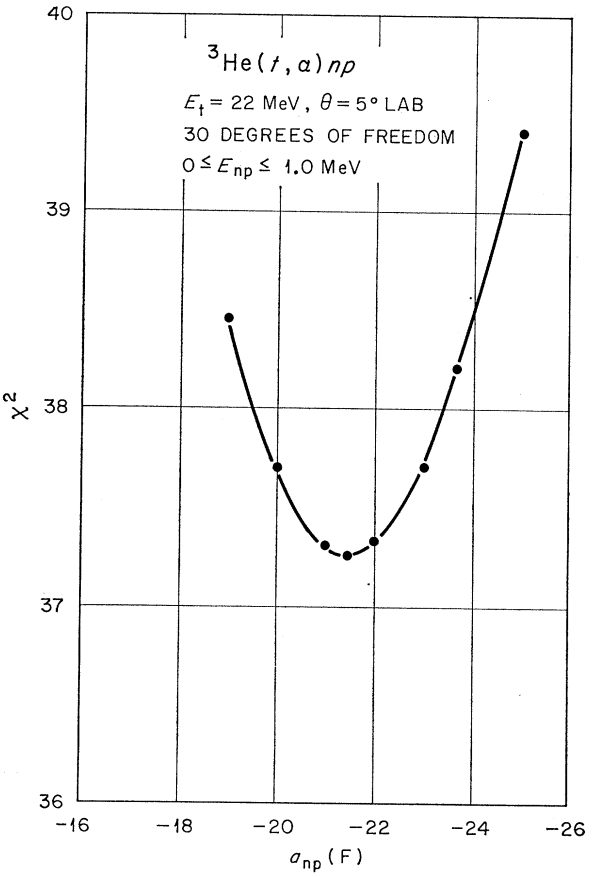

FIG. 12. χ^2 versus a_{np} for the data of Fig. 7 in the energy range $0\leq E_{np}\leq 1$ MeV. The effective range has been fixed at $r_0=2.84$ F. In the calculation of χ^2, the calculation is normalized to the total number of observed counts and the energy is allowed to shift to minimize χ^2.

B. ^{3}He(t, α)np

The minimum χ^2 fit to the n-p final-state data using the Watson-Migdal theory [Eq. (4)] is shown as the solid curve in Fig. 7. The data are only fit in the range $0\leq E_{np}\leq 1.0$ MeV because of the background uncertainties above 1.0 MeV. However, this energy interval contains much of the shape of the final-state "peak" in contrast to the p-p final-state "peak" (Fig. 3) where the peak value is just reached at $E_{pp}\approx 0.75$ MeV. This feature of the data is a consequence of Coulomb repulsion present in the p-p system and absent in the n-p and n-n systems.

The variation of χ^2 with a_{np} is presented in Fig. 12 from which we obtain $a_{np}=-21.5\pm2.3$ F. This agrees with the value $a_{np}=-23.715\pm0.013$ F for the $^1S_0$ scattering length deduced from free n-p scattering.[37] We do not know the contribution of the $^3S_1$ n-p interaction to these data although a density-of-states calculation[38] indicates that the $^3S_1$ contribution is down an order of magnitude from the $^1S_0$ contribution for the reaction $D(p, 2p)n$. All we can say is that the data are well described by the Watson-Migdal analysis and a dominant $^1S_0$ n-p interaction.

C. ^{3}H(t, α)nn

The best fit to the 5° data for this reaction is shown as the solid curve of Fig. 10. In this fit, the effective range was fixed at the value 2.84 F. The sensitivity of these data to the effective range as well as to the scattering length is illustrated by the top half of Fig. 13 which shows the $\chi_{\min}^2+1$ contour. Using Fig. 13 to determine effective-range parameters would lead to a scattering length of $a_{nn}=-17.4\pm1.8$ F and an effective range of $(r_0)_{nn}=2.4\pm1.5$ F. Thus, these data do not sensitively determine the effective range, at least with the statistics present in this experiment. We prefer to fix the effective range at the reasonable value 2.84 F which results in the χ^2 surface shown in the bottom half of Fig. 13 and a scattering length of $a_{nn}=-16.96\pm0.51$ F.

Another approach to the analysis of these data is the comparison method.[14,15] In this method, we use the ^{3}He(^{3}He, α)pp data and the known scattering parameters for two protons to "correct" the ^{3}H(t, α)nn data. In Sec. IV A, we found a two-proton scattering length of -7.52 ± 0.22 F in agreement with the known value[18]

[37] J. C. Davis and H. H. Barschall, Phys. Letters **27B**, 636 (1968).

[38] A. Niiler, C. Joseph, V. Valković, W. von Witsch, and G. C. Phillips, Phys. Rev. **182**, 1083 (1969).

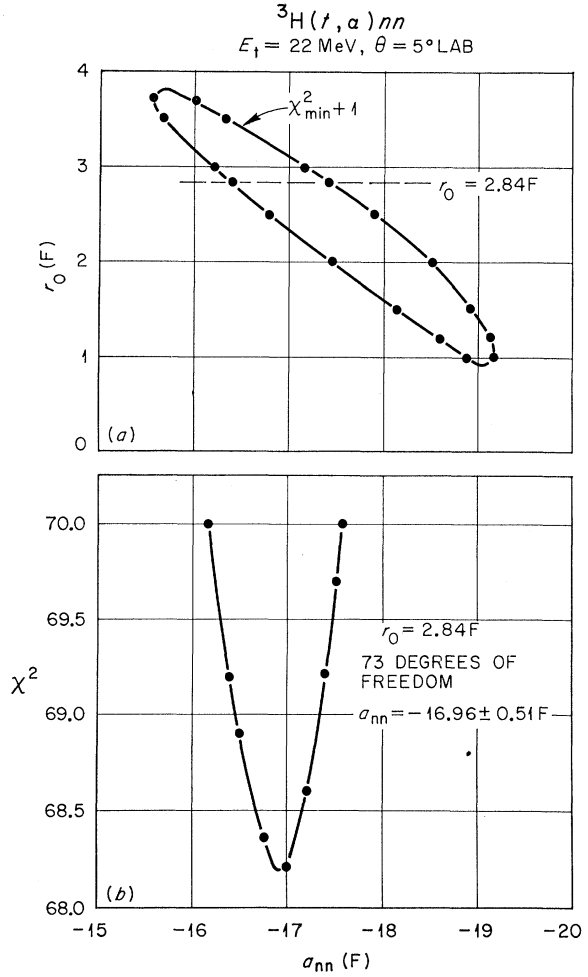

FIG. 13. The upper part of the figure (a) shows the χ_{min}^2+1 surface for the data of Fig. 10. Here the effective range r_0 and the scattering length a_{nn} are allowed to vary. Each point on this contour also includes the contribution to an uncertainty in the absolute beam energy. A slice through the χ^2 surface at $r_0=2.84$ F and viewed from the a_{nn} axis is shown in the lower half (b) of the figure.

-7.786 ± 0.008 F. Taking the value $a_{pp}=-7.52$ F seriously we can generate a "correction" factor for the *n-n* final-state data. The "correction" factor is the ratio of the Watson-Migdal expression [Eq. (4)] for the two values of a_{pp}. Searching on the *n-n* final-state data "corrected" in this way we find the value $a_{nn}=-18.11\pm0.75$ F where the error includes a contribution from an uncertainty in the "correction" factor.

V. SUMMARY AND CONCLUSIONS

We have measured the 5° α-particle spectra from the reactions ^{3}He(^{3}He, α)*pp*, ^{3}He(t, α)*np*, and ^{3}H(t, α)*nn* at a c.m. energy = 22.6 MeV in the final state. For energies less than 2 MeV in the final-state two-nucleon system, we find the α spectra to be well represented by the Watson-Migdal formalism and the known $^1S_0$ scattering parameters for the *p-p* and the *n-p* system. Applying this same formalism to the *n-n* final-state data we find $a_{nn}=-16.96\pm0.51$ F for the di-neutron scattering length when the effective range is held fixed at $r_0=2.84$ F. Allowing the data to determine the effective range as well as the scattering length, we find $a_{nn}=-17.4\pm1.8$ F and $(r_0)_{nn}=2.4\pm1.5$ F. Although not a very precise determination of the two-neutron effective range, it is one of the few such determinations and agrees with the two-proton effective range,[18] $(r_0)_{pp}=2.840\pm0.008$ F. If the *n-n* scattering length is fixed at the value -17.0 F and the χ^2 contour of Fig. 13 used to determine the effective range, we would find $(r_0)_{nn}=2.75\pm0.35$ F which is also consistent with charge symmetry. Using the *p-p* final-state data to "correct" the *n-n* final-state data in the spirit of the "comparison" method, we find $a_{nn}=-18.11\pm0.75$ F. These values for the *n-n* $^1S_0$ scattering length are to be compared with the Coulomb-corrected $^1S_0$ scattering length for two protons,[7] -17.25 F$\geq$"a_{pp}"$\geq$17.58 F. We conclude that the two scattering lengths are the same to about 1 F in 17 F. This implies[39] that the nuclear potential depth for the *n-n* system is the same as that for the *p-p* system to about 1 part in 170, the precise value being model-dependent.[19] The 5-F difference between a_{nn} and a_{np} found here would imply[39] a breakdown of charge independence of about 4%.

Finally, it is pointed out that the measured yields for the processes ^{3}He(^{3}He, α)*pp* (Fig. 3) and ^{3}H(t, α)*nn* (Fig. 10) are also consistent, within experimental error, with charge symmetry. Although the *n-n* data rise to a larger-peak cross section (because of the absence of Coulomb forces) the integrated cross section out to a relative energy of 2 MeV is the same as for the *p-p* data.

ACKNOWLEDGMENTS

For initial encouragement to use the Los Alamos facilities, we are indebted to R. F. Taschek. We wish to thank R. L. Henkel and the crew of the LASL Tandem Accelerator for making the tritium-beam exposures a success. We are similarly indebted to A. W. Riikola and the ORIC crew for the ^{3}He-beam exposures. The engineering design work of A. W. Alexander was responsible for the flawless performance of the tritium-gas target and gas-handling system. J. E. Simmons kindly lent us his tritium-gas furnace for filling the target. We are grateful for the competent assistance of R. W. Rutkowski, W. J. Roberts, and J. J. Menet during the ^{3}He exposures, and for much of the plate scanning we are indebted to Mona Leake. Finally, we wish to acknowledge the steady support and encouragement of A. Zucker and R. S. Livingston throughout the course of this work.

[39] E. M. Henley, in *Isobaric Spin in Nuclear Physics*, edited by John D. Fox and Donald Robson (Academic Press Inc., New York, 1966), p. 3.